fortune Journals

Research Article

FORTUNE JOURNAL OF HEALTH SCIENCES

ISSN: 2644-2906

Development of a Novel Thermal Technique for Detection of Water in Solvents

Joe Kirkup[*, 1, 2], Prab Birdi[2], Phil Radford[2], Kam Chana[1, 2]

Abstract

Accurate measurement of water concentration in various common solvents presents significant challenges due to the limitations of traditional detection methods, including low throughput and high costs. This study introduces a novel thermal detection technique, the LiquiSensor probe, designed for low-cost, rapid, and accurate quantification of water concentration in ethanol. The measurement principle utilizes differential thermal responses across a range of water concentrations (0-30%) in ethanol, combined with a reverse interval partial least squares (iPLS) regression model. In blind benchtop trials, LiquiSensor demonstrated accuracy within <1% of the actual water concentrations, with a standard deviation of 0.107%, indicating excellent precision, and a measurement time of only 10 minutes for multiple readings (with potential for reduction). This rapid response time, coupled with high accuracy and precision, presents significant opportunities for in-situ process monitoring as well as benchtop quality control.

Keywords: Process Analytical Technique, PAT, Water-Solvent, Ethanol, Contamination, Drying, Quality Control, QC

Introduction

Accurate quantification of the concentration of water in solvents is critical across a wide range of industries, including fuel production, fine chemicals manufacturing, and pharmaceutical development. In these sectors, minor deviations in water content can significantly impact production. For example, water concentration can affect the reaction yield or production rate of active pharmaceutical ingredients (APIs) [1], lead to the formation of undesirable by-products, alter the selectivity of extraction processes, and equilibrium parameters [2]. Consequently, precise and reliable measurement of water in solvent mixtures is essential for maintaining product quality and process efficiency. Several techniques currently exist to measure water concentration in solvents, including Karl Fischer titration [3], [4], infrared (IR) spectroscopy [5], [6], [7], and nuclear magnetic resonance (NMR) spectroscopy [8], [9]. Karl Fischer titration is the most prolific methods due to its relatively high accuracy and specificity for water detection [10]. However, it is non-portable and a time-consuming - taking 10 minutes per reading via the standard method - labor-intensive process that requires regular calibration and reagent preparation, making it less suitable for real-time, on-line monitoring in industrial settings [11], [12]. IR spectroscopy offers a non-invasive, rapid technique to measure water content, utilizing the strong absorbance of water in the infrared region [13]. While faster than Karl Fischer titration, IR spectroscopy is prone to interference from other solvent components and

Affiliation:

[1]University of Oxford, Department of Engineering Science, Osney Mead, Oxford, OX2 0ES, United Kingdom

[2]PrOXisense Ltd, Suite G041, Building A2, Cody Technology Park, Ively Road, Farnborough, GU14 0LX, United Kingdom

***Corresponding author:**
Joe Kirkup, University of Oxford, Department of Engineering Science, Osney Mead, Oxford, OX2 0ES, United Kingdom.

Citation: Joe Kirkup, Prab Birdi, Phil Radford, Kam Chana. Development of a Novel Thermal Technique for Detection of Water in Solvents. Fortune Journal of Health Sciences. 8 (2025): 92-98.

Received: January 14, 2025
Accepted: January 20, 2025
Published: February 13, 2025

may suffer from reduced accuracy at lower concentrations; although [7] demonstrated a standard deviation of <0.2% for water-ethanol concentrations of 1-19%. NMR spectroscopy, although being highly precise, is often too expensive and complex for routine use in many industrial applications, as it requires specialized equipment and expertise. Despite the availability of these techniques, many present significant challenges for widespread industrial adoption. Some, like NMR, are prohibitively expensive, while others, such as Karl Fischer titration, are not practical for continuous monitoring in dynamic process environments. These limitations highlight the need for a cost-effective yet accurate sensor capable of real-time monitoring in industrial conditions. The focus of this research is to address the identified gap by developing a process sensor capable of discriminating liquid concentrations in a binary solvent system. Specifically, the research aims to detect and quantify water concentration in ethanol across a range of representative concentrations. The performance of the sensor has been evaluated in terms of accuracy, precision, bias, and linearity. The authors seek to contribute to the development of more affordable and effective monitoring tools for industrial applications.

Sensor Background & Theory

Sensor Design & Data Acquisition

At the core of the sensor's design is a cylindrically symmetrical active portion, engineered to produce a radially uniform heat flux. Achieved by applying an electrical square wave pulse, which causes controlled heat dissipation into the surrounding sample material. The rate at which heat dissipates varies depending on the chemical composition of the sample, reflecting the thermal properties of the substance. Specifically, changes in heat dissipation correspond to variations in thermal properties such as thermal conductivity and specific heat capacity. These thermal interactions result in a distinct temperature profile, or trace, along the sensor's sleeve. To capture thermal response, an embedded temperature sensor is strategically placed within the sensor assembly. The sensor continuously monitors the temperature changes during and after the pulse, providing a real-time temperature trace. Data is transmitted to a proprietary processing box - connected to and powered by a data acquisition laptop via USB-C - which interfaces with bespoke data acquisition and analysis software. The software processes the recorded temperature traces, which are entered into a statistical model which produces a concentration prediction. This process is captured in Figure 1.

Measurement & Modelling Principles

The primary analytical parameter that characterises the difference between various sample compositions is the thermal product, also known as thermal effusivity. Effusivity

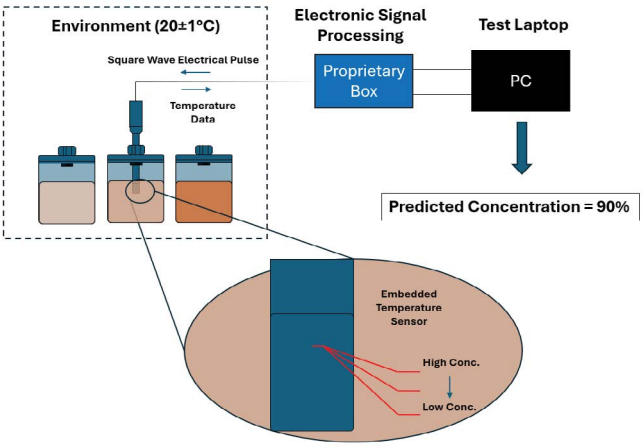

Figure 1: Simplified representation of the LiquiSensor measurement process, highlighting the core measurement principle.

is a material property that quantifies a material's ability to exchange heat with its surroundings. It describes how readily a material absorbs or rejects heat and is mathematically defined as

$$e = \sqrt{\rho C_p k} \quad (1)$$

where ρ is the material's density, C_ρ is the specific heat capacity, and k is the thermal conductivity. Together, these factors determine the rate at which a material responds to thermal changes, making thermal effusivity a key characteristic in understanding the thermal interaction between the sensor and its environment. A commonly used method for measuring thermal effusivity involves exciting a thin metallic strip on a semi-infinite substrate with an electrical square wave pulse. This method is based on fundamental work by [14] for instrumentation measuring transient heat flux in hypersonic short-duration facilities, which was adapted by multiple authors including [15], [16], [17] to measure thermal effusivity and other properties correlated with material characteristics. The temperature response of the material under these conditions is governed by the 1D heat conduction equation, which models the temperature change over time and space.

$$\frac{\partial T}{\partial t} = \alpha \frac{\partial T^2}{\partial x^2} \quad (2)$$

where $\alpha = \frac{k}{\rho C_p}$ is known as the thermal diffusivity. Applying a series of semi-infinite assumptions, Laplace transforming, solving for the transfer function, multiplying by the Heaviside step function, and transforming back into the time domain produces equation (3) relating the heat flux (Q) to the thermal effusivity via the temperature change from initial to final (ΔT):

$$Q = \frac{\sqrt{\pi}}{2} \frac{e}{\sqrt{t}} \Delta T \quad (3)$$

Joe Kirkup, et al., Fortune J Health Sci 2025
DOI:10.26502/fjhs.257

LiquiSensor extends the traditional approach to thermal product measurement by interrogating both the heating and cooling phases of the process. Instead of focusing solely on the resistance change during the electrical pulse as in the conventional methods, LiquiSensor captures the full temperature trace across both phases, allowing for a more comprehensive analysis of the thermal behaviour of materials and their corresponding thermal properties. Unlike previous methods that rely primarily on analytical or regression-based models for interpreting thermal data, LiquiSensor adopts a chemometric approach. Chemometrics refers to the application of mathematical and statistical techniques to extract useful information from complex chemical data. This approach enables a more nuanced interpretation of the temperature traces by accounting for the multidimensional nature of the data and identifying underlying patterns that are not evident with traditional analysis methods. Futhermore, the method enables the creation of predictive models that can be used to correlate thermal data with specific material properties, including composition, phase changes, and reaction kinetics. Such predictive capabilities are invaluable in industrial settings, where real-time monitoring and rapid decision-making are critical. By combining thermal effusivity with advanced data analysis techniques, LiquiSensor represents a significant advancement in the field of thermal product measurement. It not only builds on the established principles of heat dissipation and temperature monitoring but also integrates cutting-edge statistical methods to extract more meaningful insights from the data.

Material and Methods

Sample Preparation

Absolute ethanol (ReAgent Ethyl Alcohol) and purified water (Pure Klenz Purified Water EP) were used to create the model samples detailed in Table 1 by-weight, using a 4-place analytical balance (Kern ADB100-4A). Each sample was measured into a laboratory container (Duran GLS 80) and fitted with a sealed lid containing an access port (Duran GL18 Insert). This port enabled quick insertion/removal of the LiquiSensor probe with minimal sample disturbance, preventing evaporation of ethanol altering the actual sample concentrations. No pre-conditioning drying step of the ethanol was performed before testing.

Testing Procedure

Samples were tested on the bench non-sequentially to eliminate any bias introduced via testing order. The testing procedure involved inserting the LiquiSensor probe through the access port and connecting the electronics box to the LiquiSensor probe via the 'connector hub'. A test was then initiated via PrOXisense's data acquisition and analysis software, using a 1 second sample pulse length at a sample rate of 100 Hz. This pulse is repeated 10 times, with a gap between pulses of 60 seconds and a 25 seconds sample window. After test completion, the LiquiSensor probe was removed from the sample and thoroughly cleaned with isopropyl alcohol (Trade Chemicals), a lint-free wipe (kuou), and compressed air (Anker). This process was repeated for all model samples tested. To validate measurement system accuracy, a set of blind samples - prepared in the same manner as the initial model samples, but without the operator having prior knowledge of their concentrations - was performed. The predicted concentrations from the model were compared to the actual concentrations of these blind samples to assess the model's predictive accuracy.

Data Processing & Analysis

Inspection, initial analysis, and data cleaning/formatting such as delta normalisation from the starting environmental temperature were performed at this point using MATLAB R2022a (Mathworks) to minimise absolute baseline variation. The data was loaded into Solo 9.1 (Eigenvector Research Inc.) where the bulk of the model processing occurred. The data was labelled and pre-processed via mean-centring and a 1st derivative point treatment to highlight subtle gradient

Table 1: Ethanol-water concentrations for each sample number tested.

Sample #	*Ethanol Concentration (%, w/w)*	*Water Concentration (%, w/w)*
1	100	0
2	98	2
3	96	4
4	94	6
5	92	8
6	90	10
7	85	15
8	80	20
9	75	25
10	70	30

Joe Kirkup, et al., Fortune J Health Sci 2025
DOI:10.26502/fjhs.257

differences. The first pulse in each sequence of 10 was omitted, as it was considered a 'warm-up' pulse to establish an appropriate temperature gradient within the active portion and (during pre-trials) decreased measurement accuracy. A reverse iPLS (interval partial least squares) regression was performed, with a specified interval size of 100 samples, automatic step size, and automatic interval number. Cross-validation was performed using a Venetian blinds scheme (n = 9). Metrics such as RMSECV and R-Squared were automatically calculated by Solo 9.1 for the model produced. The blind samples were subsequently processed as described above. Metrics comparing the actual blind concentrations and their respective predicted concentrations were calculated. Performance metrics such as standard deviation as an indicator of precision were performed using MATLAB R2022a (Mathworks).

Results & Discussion

Raw Temperature Traces

Figure 2 shows the mean average temperature trace of each sample over time.

The thermocouple temperature rises from a starting point of $\Delta T = 0^{\circ}C$ at t = 0s to approximately $\Delta T = 15^{\circ}C$ at t = 1s as a result of resistive heating from the electrical square wave pulse. The sensor input power and duration were chosen in previous testing to elicit a consistent $\Delta T = 15^{\circ}C$ temperature rise in water, therefore these trace characteristics confirm the chosen sensor was repeatable and functioned as intended. Relying on visual inspection alone, the heating portion of the trace appears identical for all tested samples. As the thermocouple temperature decays in the cooling portion, the trace for each sample diverges from t = 1s − 6s; during which a clear pattern of higher concentration ethanol samples decaying slower than lower concentration ethanol samples is clearly noticeable. This trend aligns with the solvents relative thermal effusivity as seen in Table 2, with the trace separation at t = 4s − 7s being approximately linear with sample ethanol concentration levels. From this correlation it is clear that this technique may hold predictive power; however in order to refine and quantify this, additional statistical processing was required.

Baseline Statistical Model

The reverse iPLS analysis approach allowed for a more focused analysis of the most relevant temperature

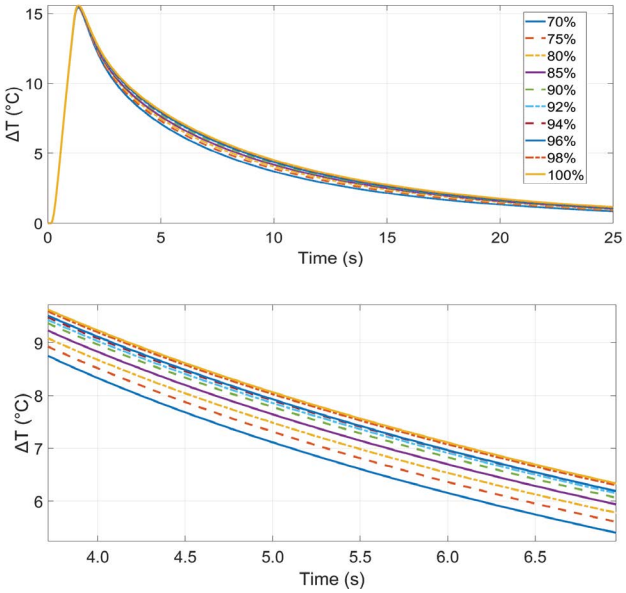

Figure 2: Above: Raw thermocouple temperature against time for different EtOH-Water sample concentrations; Below: Zoom-in on t = 4s - 7s where the traces begin to noticeably diverge.

trace regions, reducing model complexity, improving interpretability, and predictive power. The advantages can be clearly seen in Figures 3 - 4, which detail the temperature trace regions giving rise to the greatest sample variation and the weightings of each latent variables (LVs) time-point in the temperature trace, respectively.

Figure 3 indicates that selecting a window of t = 1s − 3s (inflection region) and t = 6s − 7s (separation region) gave the superior prediction (i.e. the lowest RMSECV for a 100 sample interval) after an exhaustive search. The regions identified have either clear temperature trace characteristics or can be linked to the environments thermal characteristics:

Inflection Region - Inclusion of this region is likely linked to the physical mechanism of capturing transient variation in thermal inertia. The short duration after abruptly ending the electrical heating pulse could amplify thermal effusivity differences of the sensor's environment.

Separation Region - The sample temperature traces show the greatest variation and linearity later in the pulse; therefore, this is a logical inclusion in the model. This is the region of the temperature trace where the difference in the temperature 'driving-force' over time between each sample

Table 2: Typical thermal properties of the test solvents at approximate standard conditions (20◦C; 1.01325 kPa)

Material	*Mass Density (kg/m³)*	*Isobaric Specific Heat Capacity (J/kg°C)*	*Thermal Conductivity (W/m°C)*	*Thermal Effusivity ($J/m^2s^{0.5}°C$)*
Water	1000	4.18	0.6	50.1
Ethanol	791	2.49	0.16	17.8

Citation: Joe Kirkup, Prab Birdi, Phil Radford, Kam Chana. Development of a Novel Thermal Technique for Detection of Water in Solvents. Fortune Journal of Health Sciences. 8 (2025): 92-98.

Joe Kirkup, et al., Fortune J Health Sci 2025
DOI:10.26502/fjhs.257

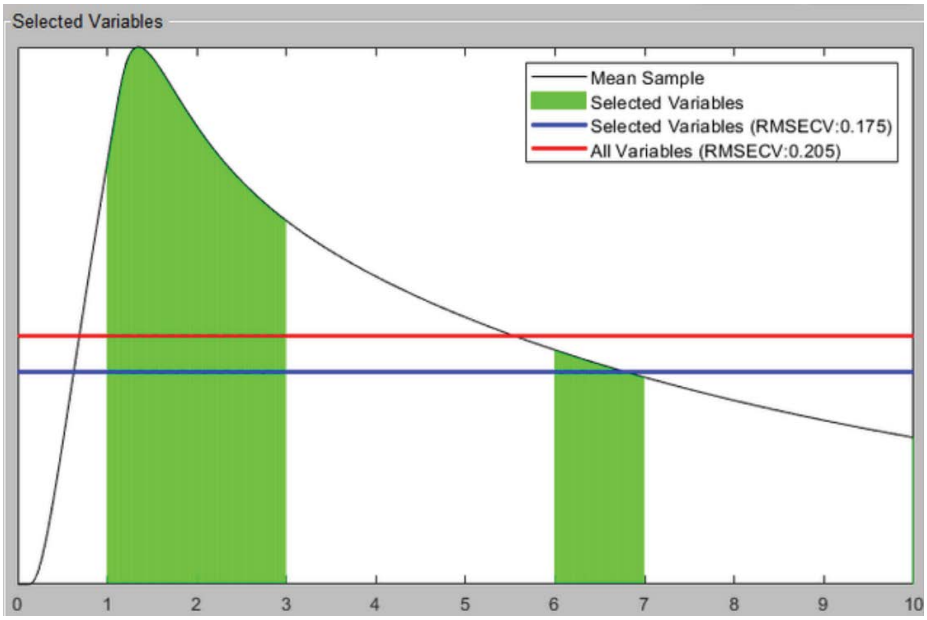

Figure 3: Windows of variables selected via the reverse interval process as giving rise to the greatest variation in the tested samples.

reached its maximum. Later periods in the pulse result in reduced variation as samples are cooling back to a common baseline environmental temperature.

Having identified possible physical mechanisms for the interval window selections and as a result of the short-duration of transient thermal inertia, the model maybe improved by examining the effect of varying the interval size window. This would enable Solo 9.1 to capture shorter-duration sample differentiating events without including extra time-points that do not contribute to sample variation. The ideal window size would be the duration of the shortest sample differentiating thermal event without the selected variable window significantly fragmenting (which would be indicative of fitting measurement noise). Examining Figure 4, LV 1 accounted for the majority of the variability (as expected) capturing 86.84% of the observed variance. The weightings clearly resemble the temperature profile, which (in combination with the pre-processing steps) re-enforce that the gradient of the heating phase peak and the gradient at maximum divergence are critical. LV 2, LV 3, and LV 4 accounted for 1.60%, 1.95%, and 0.35% of the variance respectively; which is somewhat lower than expected and is more challenging to interpret physically. They do however, contribute to a significant increase in model performance decreasing RMSECV from 0.1692 to 0.1502; therefore they have been included. Adding additional LVs does not significantly increase the RMSECV and can be considered random statistical noise.

A plot of the actual nominal EtOH concentration against the predicted EtOH concentration produced from the 4 LV regression model can be seen in Figure 5.

The model exhibited strong predictive capabilities with an RMSEC = 0.073, and an RMSECV = 0.150. These low error values demonstrate the model's ability to generalise across different sample sets, indicating robust predictive performance. Furthermore, the model response was highly linear, with an R^2 = 1.00 (2 d.p) for both the calibration and cross-validation data.

Blind Test Prediction

In the blind testing phase, the model demonstrated impressive prediction accuracy, with the predicted ethanol concentrations being within 1% of the actual nominal concentrations. Table 3 shows the actual and measured concentrations for each sample. Moreover, the standard deviation within individual sample repeats was 0.107%, highlighting the reproducibility and precision of the sensor.

One notable outcome from the analysis was the observation of a systematic overprediction bias. This can be corrected in future models by applying a bias correction factor, through pre-processing optimization, or the examination of the data via alternative modelling techniques such as support vector machines. However, as we are comparing the predicted EtOH concentration to the nominal concentration when calculating our measurement error, what appears to manifest as overprediction bias in LiquiSensor may be present in the samples as a result of systematic error in the analytical

Joe Kirkup, et al., Fortune J Health Sci 2025
DOI:10.26502/fjhs.257

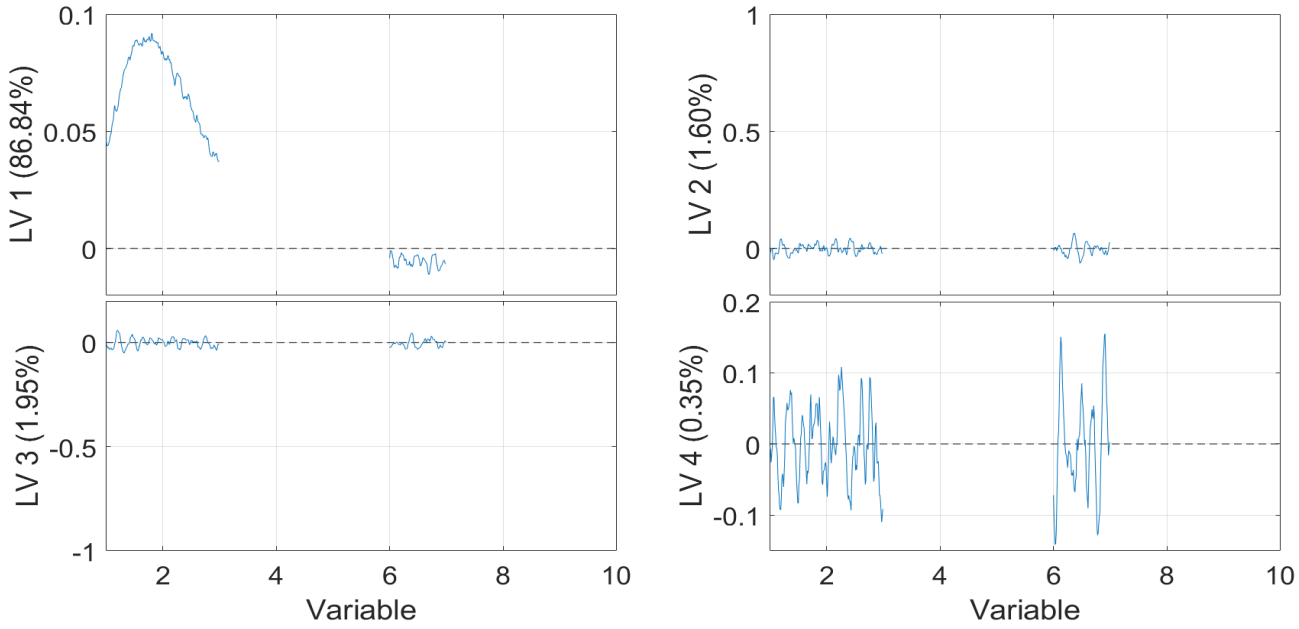

Figure 4: Variable weightings for LV 1 (top left), LV 2 (top right), LV 3 (bottom left), and LV 4 (bottom right). The percentage of overall sample variance accounted for by each LV is provided in the y-axis.

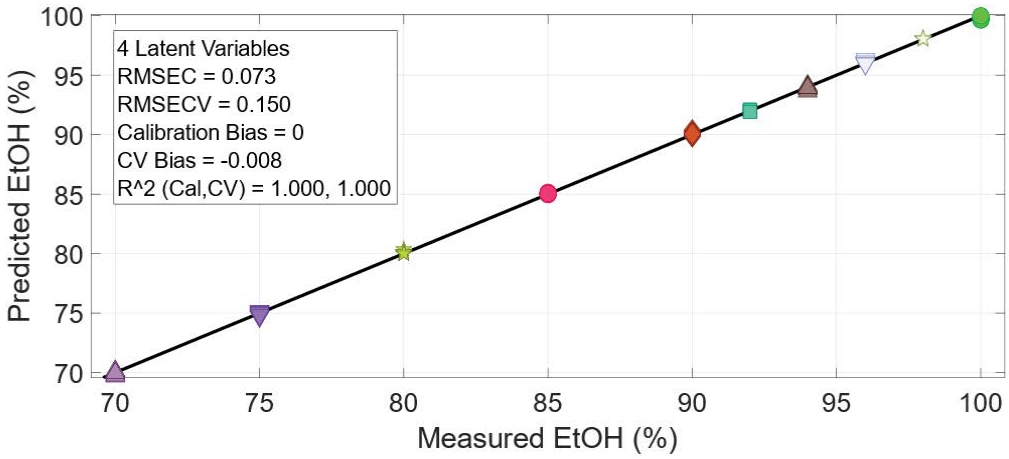

Figure 5: Nominal EtOH concentrations plotted against the EtOH predictions from the reverse iPLS model.

Table 3: Results table detailing the error between the nominal concentration of EtOH and the concentration predicted by LiquiSensor.

Sample #	*Actual Ethanol Concentration (%, w/w)*	*Predicted Ethanol Concentration (%, w/w)*	*Error From Nominal (%, w/w)*
1	100	100.65	0.65
2	98	98.64	0.64
3	93	93.67	0.67
4	88	88.79	0.79
5	79	79.91	0.91

balance and/or operator error. In future validation testing, it is therefore advised to test against a standard method such as Karl Fischer titration or IR spectroscopy with characterised performance to identify the magnitude of inaccuracy introduced.

Conclusion

The results demonstrate the effectiveness of the LiquiSensor sensor combined with iPLS regression in quantifying blind tested ethanol-water concentrations with high accuracy (within 1%) and precision (average 0.107%). The robustness and generality of the model - as indicated by the RMSECV of 0.150 - coupled with its strong linearity

(R-Squared (CV) = 1.000) suggests that, with further development, this approach could be highly valuable for real-time monitoring in-line for industrial applications as well as for laboratory benchtop analysis. Refinement of the model to correct the overprediction bias will further enhance performance; and examination of LiquiSensor's predictive capabilities over a wider ethanol-water concentration range and environmental conditions are required to fully capture the required performance envelope. Benchmarking against a fully characterized technique is also recommended.

Acknowledgements

The authors of this document would like to acknowledge Michelle Cardwell, Jay Thethi & Amelia Claxton of PrOXisense Ltd. for their help during the experimental investigation phase of the work.

Conflicts of Interest

No conflicts of interest were declared.

References

1. Salmar S, Järv J, Tenno T and Tuulmets A. "Role of water in determining organic reactivity in aqueous binary solvents," Central European Journal of Chemistry 10 (2012).
2. Srour RK and McDonald LM. "Solution properties of inorganic contamination in mixed solvents: Theory, progress, and limitations," Crit Rev Environ Sci Technol 41 (2011).
3. Schöffski K and Strohm D. "Karl Fischer Moisture Determination," Encyclopedia of Analytical Chemistry (2000).
4. Rivera-Quintero P, Patience GS, Patience NA, Boffito DC, Banquy X et al. "Experimental methods in chemical engineering: Karl Fischer titration," Can J Chem Eng 102 (2024): 2980–2997.
5. Ludvík J, Hilgard and Volke J. "Determination of water in acetonitrile, propionitrile, dimethylformamide and tetrahydrofuran by infrared and near-infrared spectrometry," Analyst 113 (1988): 1729–1731
6. Barbetta A and Edgell W. "Infrared Spectrophotometric Determination of Trace Water in Selected Organic Solvents," 32 (1978): 93–98.
7. Cho S, Chung H, Woo YA and Kim HJ. "Determination of water content in ethanol by miniaturized near-infrared (NIR) system," Bull Korean Chem Soc 26 (2005).
8. Creary X. "No-Deuterium Proton (No-D) NMR as a Convenient Method for Analysis of Organic Solvents," Journal of Organic Chemistry 88 (2023): 11545–11551.
9. Wan K, et al., "Accurate Determination of Trace Water in Organic Solution by Quantitative Nuclear Magnetic Resonance," Anal Chem 95 (2023): 15673–15680.
10. Connors KA. "The Karl Fischer Titration of Water," Drug Dev Ind Pharm 14 (1988): 1891–1903.
11. Tavar E, Turk E and Kreft S. "Simple modification of karl-fischer titration method for determination of water content in colored samples," J Anal Methods Chem 1 (2012).
12. Ronkart SN, Paquot M, Fougnies C, Deroanne C, Van Herck JC and et al. "Determination of total water content in inulin using the volumetric Karl Fischer titration," Talanta 70 (2006).
13. Bär D, Debus H, Brzenczek S, Fischer W and et al. "Determining particle size and water content by near-infrared spectroscopy in the granulation of naproxen sodium," J Pharm Biomed Anal 151 (2018): 209–218.
14. Schultz DL and Jones TV. "HEAT-TRANSFER MEASUREMENTS IN SHORT-DURATION HYPERSONIC FACILITIES" AGAR Dograph 165 (1973).
15. Chana K. "Thermal Product Sensor: A potentially new diagnostic tool in the detection of skin malignancy.," Med Res Arch 12 (2024).
16. Sridhar V, Chana KS and Singh D. "Computational and experimental study of a platinum thin-film based oil condition and contamination sensor," in Proceedings of the ASME Turbo Expo (2017).
17. Sains P, Chana KS, Sridhar V and Sajid MS. "Pilot study on an innovative biosensor with a range of medical and surgical applications," BMC Res Notes 11 (2018).